Polarization-independent blue-phase liquid-crystal gratings driven by vertical electric field

Ge Zhu
Jia-nan Li
Xiao-wen Lin
Hai-feng Wang
Wei Hu (SID Member)
Zhi-gang Zheng
Hong-qing Cui
Dong Shen
Yan-qing Lu (SID Member)

Abstract — A blue-phase liquid-crystal grating is proposed by applying a vertical electric field with lateral periodic distribution. Simulation on electric-field distribution was also carried out, the results of which suggest the alternation of isotropic and ordinary refractive indices in the lateral direction. Through the electrode configuration design, both 1D and 2D gratings were demonstrated with high transmittance of ca. 85%. The diffraction efficiency of the first order reached up to 38.7% and 17.8% for the 1D and 2D cases, respectively. The field-induced fast phase modulation permits a rapid switching of diffraction orders down to the submillisecond scale.

Keywords — *Liquid-crystal grating, blue phase, vertical field, polarization independent.*
DOI # 10.1889/JSID20.6.341

1 Introduction

The past half-century has witnessed the tremendous development and comprehensive applications of liquid-crystal (LC) technologies. LC has now been widely used not only in the display field[1–4] but also as very important tunable passive components[5–10] because of their advantages of light weight, low cost, no moving parts, and low power consumption. A switchable phase grating is one type of such components. Since Carroll first proposed the idea of LC diffraction grating,[11] extensive work has been performed on this topic. To form the grating profile, a periodical refractive-index change of LC is required. There have been several strategies to realize such a profile, among which two ways are most commonly used. The first is to form a periodical electric-field distribution by the design of the electrode configuration. Striped[12,13] or interdigitated[14] electrodes on one or both substrates of the LC cells were proposed and demonstrated, generating a non-uniform electric field and thus forming the grating profile. The second is to directly guide the initial LC directors to realize periodicity in the refractive index. It can be divided into two aspects: one is to form patterned alignment layers through either mechanical contact methods[15] or photoalignment techniques[16,17]; the other is the holographic recording technologies on polymer-dispersed liquid crystal (PDLC).[18–20] However, in most of these approaches, conventional nematic LC materials are employed, but some problems such as low diffraction efficiency and slow response time need to be further improved.

In the previous 10 years, polymer-stabilized blue-phase liquid crystal (PSBPLC)[21] has become an emerging promising candidate for either display[22–25] or photonic applications.[26,27] The unique structure of this material permits two major desiring features: no need for alignment layers and a fast response time down to the submillisecond range. Based on this attractive LC material, a high efficiency and fast-response tunable phase grating has recently been demonstrated by Yan *et al.* through the use of in-plane switching (IPS).[28] Most recently, a 1D/2D switchable BP grating was demonstrated by Zhu *et al.* based on selective IPS driving on both substrates.[29]

Herein, we proposed the use of a vertical field with periodic lateral distribution to form a grating profile of PSBPLC and demonstrated both 1D and 2D tunable gratings based on this idea. Besides the properties of high efficiency and fast switchability, our grating also possesses the characteristic of polarization independency, attributed to the vertical field. Simulation on the electric-field distribution was carried out that agreed well with the experimental results.

2 Principle and device configuration

BP I and II are the most commonly used phases of BPLCs, with double-twist self-assembled LC cylinders stacked in three dimensions forming cubic symmetry.[30–32] The structural symmetry induces optical isotropy of BPs. Polymer stabilization is now commonly utilized to broaden the BP temperature range.[21] At the voltage-off state, the refractive index of PSBPLC is defined as n_{iso} [Eq. (1)].[33] When an electric field is applied, birefringence is induced according

G. Zhu, J. Li, X. Lin, W. Hu, and Y. Lu are with Nanjing University, College of Engineering and Applied Sciences and the National Laboratory of Solid State Microstructures, 22 Hanlou Rd., Nanjing, Jiangsu 210093 P.R. China; telephone +86-25-8359-5535, e-mail: huwei@nju.edu.cn.
H. Wang, Z. Zheng, and D. Shen are with East China University of Science and Technology, Department of Physics, Shanghai, P.R. China.
H. Cui is with Infovision Optoelectronics Corp., LCD R&D Center, Kunshan, P.R. China; telephone +86-21-6425-3514, e-mail: zgzheng@ecust.edu.cn

to the Kerr equation.[34] The refractive-index changes can be expressed as Eqs. (2) and (3):

$$n_{iso} = \frac{2n_o(E) + n_e(E)}{3}, \quad (1)$$

$$\delta n_o(E) = n_{iso} - n_o(E) = \frac{n_e(E) - n_o(E)}{3}, \quad (2)$$

$$\delta n_e(E) = n_e(E) - n_{iso} = \frac{2n_e(E) - 2n_o(E)}{3}, \quad (3)$$

where $n_o(E)$ and $\delta n_o(E)$ are the field-dependent refractive index and index change perpendicular to the electric field, while $n_e(E)$ and $\delta n_e(E)$ are those parallel to the electric field. The dependence of induced birefringence $\delta n(E)$ on the external field could be obtained by using the extended Kerr equation, which is an exponential-convergence-model-based equation proposed by Yan *et al*:[33]

$$\delta n(E) = n_e(E) - n_o(E) = \delta n_{sat}\left(1 - \exp\left[-\left(\frac{E}{E_s}\right)^2\right]\right). \quad (4)$$

Here, δn_{sat} represents the saturated birefringence and E_s the characteristic saturation field. The extended Kerr equation fits the experimental data very well in the entire field region.

In this work, we present a PSBPLC switchable grating with striped electrodes at least on one side. The electrodes are employed to generate a vertical electric field with a lateral periodic field-intensity distribution. According to the Kerr effect, a refractive-index change occurs cyclically on each electrodes' covered region, but does not occur at gap domains. This indicates alternating ordinary and isotropic refractive indices that are exhibited laterally, despite the polarization of the incident light, providing a polarization-independent phase-grating profile.

Through electrode-configuration design, both 1D and 2D gratings could be accomplished. In Fig. 1(a), a cell with a 10-μm electrode width and 10-μm gap on one side and a planar electrode on the other side was presented (cell gap is 12 μm). An achromatic light beam is normally incident to the cell. At the OFF-state, LC refractive indices in the two alternating regions are uniform as n_{iso}; therefore, no diffraction could be observed. When an AC signal is applied [ON-state, as shown in Fig. 1(b)], the LC refractive index changes to n_o in the striped electrode covered regions, while that in the electrode-gap regions remains approximately unchanged. As a result, the incident light is diffracted.

2D gratings are fabricated by assembling a cell with striped electrodes on both substrates orthogonally [Fig. 1(c)]. Their behavior is the same as 1D gratings at the OFF-state. After applied voltages, the refractive index of LC on the crossed-electrode regions will change to n_o for normally incident light, while that on other regions still remains approximately as n_{iso} because the field intensity is much smaller.

Here, the phase retardation is due to the refractive-index difference between two regions (δn_o). According to Eqs. (2) and (4), δn_o is only 1/3 of δn (the induced birefringence in IPS mode). However, thanks to the vertically driven field, all LC under an applied field in the longitudinal direction (cell gap 12 μm) will contribute to δn_o instead of only a 3–5-μm penetration depth in the IPS mode. The mechanism permits this type of gratings in order to achieve comparable phase retardation as in the IPS mode.

3 Simulation and experiment

We used a BP module of the commercial software Techwiz LCD to simulate the electric-field distribution in both 1D and 2D gratings. A 1-kHz rectangular signal is used in the simulation, the same as in our experiment. And the voltage is set to 50 V_{rms}. We define the x-direction perpendicular to the striped electrodes in the plane of the substrate and z-direction perpendicular to this plane. Figures 2(a) and 2(b) show the results of 1D cases in the x–z and x–y planes, respectively, within two periods of electrodes. Figure 2(b) shows the cross section in the middle of cell as the black line labeled in (a). Only the electric field along the z-axis (E_z) is exhibited, and its intensity is scaled by the color bar. We can observe from (a) that the field intensity is strongest under the striped electrodes and gradually decreases towards the opposite planar electrode; while it is weakest at the elec-

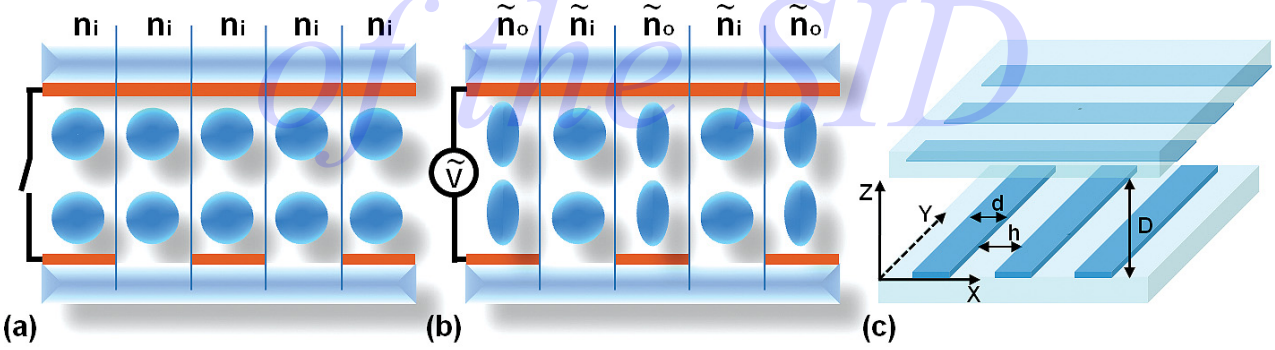

FIGURE 1 — (a) and (b) are the schematic diagrams of the effective-optical-index ellipsoids of PSBPLC in the 1D grating structure at the voltage-off and voltage-on state, respectively. (c) is the structure of the 2D grating with electrode directions on the two substrates orthogonal. The electrode width d is 10 μm, gap width h is 10 μm, and cell gap D is 12 μm.

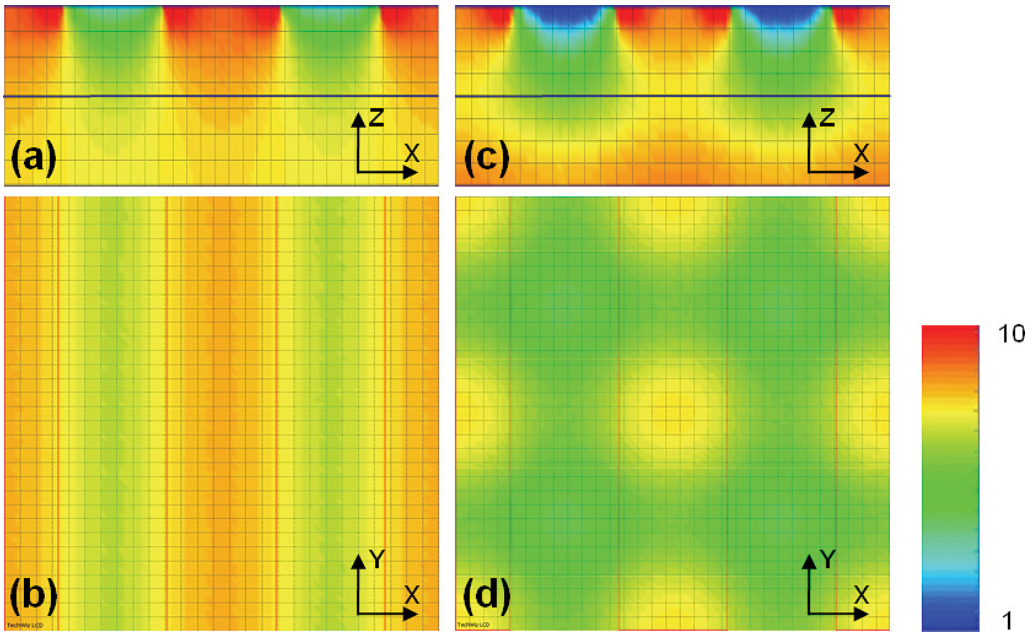

FIGURE 2 — Simulation diagrams of the electric field at 50 V_{rms} for 1D (a)-(b) and 2D (c)-(d) gratings separately. The unit of the color bar is V/μm.

trode gaps and increases towards the opposite. Figure 2(b) evidently reveals that the field distribution is coincident with the electrode design. Figures 2(c) and 2(d) are the simulation results in the 2D cases. Similar to those in the 1D cases, the field intensity is strongest in the crossed-electrode regions and weakest in the areas with no electrodes, while intermediate in single-electrode regions. Based on the simulated field distribution and BP material parameters, a theoretical prediction on the electro-optic properties is possible. Yan *et al.* have shown that the theoretical prediction matches well with experimental results in a closely related system.[28] Besides, E_z, E_x, and E_y are simulated as well, the intensity of which are negligible compared with E_z. As explained by the Kerr effect, the refractive-index distribution is directly defined by that of the electric field intensity. That is to say, a normally incident light beam only sees $n_o(E)$ in the cell, which is independent of polarization direction.

In our experiment, the PSBPLC precursor is a mixture of 93-wt.% chiral nematic liquid crystal (N*LC) host and 7 wt.% monomers. The N*LC host is composed of eutectic nematic LCs (75 wt.%, Δn = 0.168, XH-07, Xianhua Chemicals, Ltd.) and chiral dopant R811 (25 wt.%, Merck). The monomers contain two components: one is the common 2-ethylhexyl acrylate (2-EHA) and the other is $PTPTP_n$ [4-(*n*-acryloyloxypropyloxy)-benzoic acid 2-methyl-1,4-phenyleneester, mixed by $PTPTP_3$ and $PTPTP_6$ at a weight ratio of 1:1]. The weight ratio between 2-EHA and $PTPTP_n$ is 1:2. To promote the polymerization of monomers, a small amount of photoinitiator, Irgacure 184 (0.5 wt.%, Ciba), is added. The precursor is stirred above the clearing point for about 30 minutes and then capillary filled into a cell. It was kept at the isotropic phase for 15 minutes after filling to suppress the flow orientation. No alignment layers are settled in the cell. The phase-transition temperature of PSBPLC precursor is ISO 34.3°C BP 29.5°C N* during the

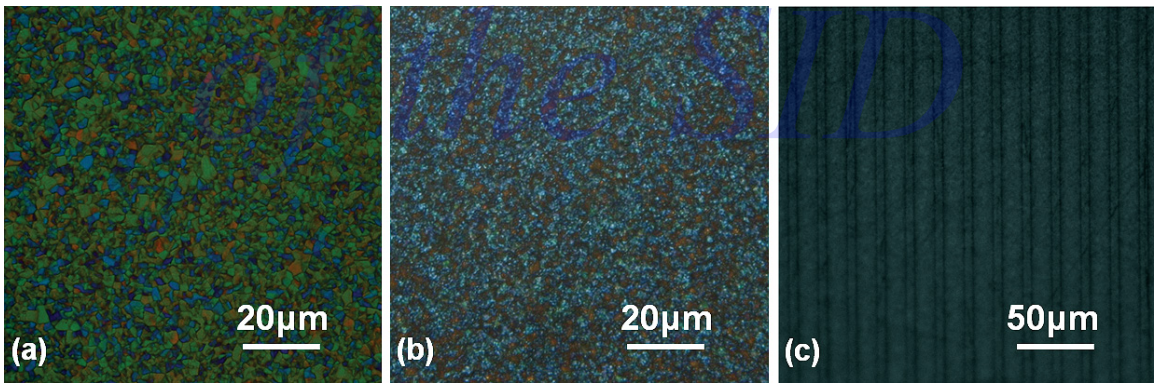

FIGURE 3 — The LC textures of BP: (a) at the initial voltage-off state and (b) immediately after a 50 V_{rms} signal was turned off and (c) the structure of 1D BP gratings as 50 V_{rms} is applied.

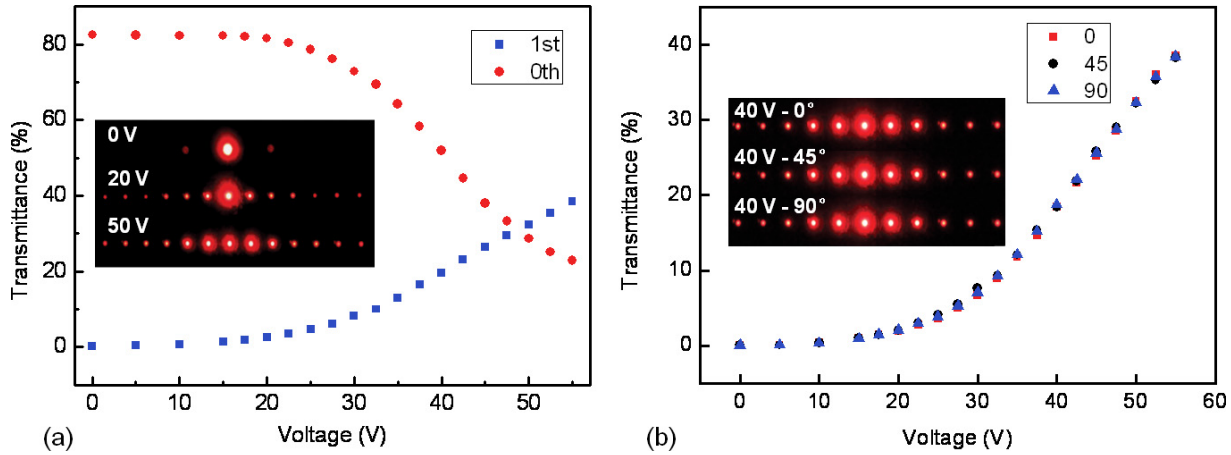

FIGURE 4 — Diffraction patterns (insets) and efficiencies of (a) zeroth and first orders; (b) first order under different polarized incident light.

cooling process at a cooling rate of 0.5 °C/min and is enantiotropic with a narrower temperature range on heating. Then the precursor is UV-cured at an intensity of 8.3 mW/cm^2 for 6 minutes. After polymer stabilization, its temperature range is extended to over 73°C (38.2°C to below –35°C).

Figure 3 shows the textures of PSBPLC (a) at the initial voltage-off state and (b) immediately after a 50-V_{rms} signal was turned off. Micrographs were taken under a polarizing microscope (Olympus BX-51) with orthogonal polarizers. Corresponding to the selective Bragg reflections of BP, color domains are observed in the images. The different colors in Fig. 3(a) are due to different orientations of the cubic lattices, which are quite random at the voltage-off state. When voltage is applied, molecules rotate to change the lattices, making its orientation more uniform. This uniformity would still remain for some time after the voltage is turned off. So the texture in (b) is less colorful than that in (a). Except for the slight difference in colors, the feature texture of BP after applying a voltage is almost unchanged. The result proves good stabilization of PSBPLC against applied voltages. Figure 3(c) reveals the structure of 1D BP gratings as voltage is applied (herein 50 V_{rms} as an example), which is coincident with the electrode design. It results from the different distortion of lattice corresponding to the periodic variations of vertical applied electric-field intensity. Lower transmittance and smaller domain size compared to the voltage-off state were observed as voltage was applied. The uniform low transmittance suggests no phase retardation is generated. It indicates that the lateral field is negligible, as expected, permitting a good polarization independency.

In our experiments, the LC cells were driven by a 1-kHz AC rectangular signal with a duty cycle of 50%. The voltage-dependent diffraction properties were tested in the below measurement setup. A light beam from a He–Ne laser (632.8 nm) passed first through a polarizer and then through a λ/4 wave plate (@633 nm). As the He–Ne laser is elliptically polarized, this step is to change it to be circular polarized. Afterwards it went through another polarizer and finally normally through the sample and was collected by a photodetector. Therefore, the polarization direction of incident light could be freely tuned just by rotating the second polarizer without changing its intensity.

4 Results and discussion

The electro-optical properties of a 1D PSBPLC grating were tested. The two curves in Fig. 4(a) show ratios of the energy collected from the zeroth and first orders divided by the total transmittance at the OFF-state, respectively. As expected, no threshold voltage is observed as the mechanism of field-induced birefringence. And the intensity variation of the zeroth-order and first-order mirrors each other as a function of applied voltage. The phase retardation has not reached one π, so that the intensity of zeroth or first order does not exhibit an extremum. However, the diffraction efficiency of the first order (defined as the ratio between the intensity of the first order and total transmitted) still reached 38.7% at 55 V_{rms}, comparable to that reported with a phase retardation of π (40% at 160 V_{rms}).[28] This indicates that the diffraction intensity here is very close to a maximum. It is coincident with our assumption in principle that the gratings receive contributions from LC molecules in the entire vertical direction. The insets in Fig. 4(a) provide some photos of diffraction patterns. The patterns follow the curves very well and directly prove the tunability of the gratings. At the voltage-off state, weak diffraction patterns could be observed due to the striped electrodes. Two comparatively strong dots appear, the reason of which is the orientation of LC molecules by the relief boundaries of electrodes, forming a grating with half the period of the original striped electrodes.

The polarization direction of incident light beams was changed, and then transmittance curves of first order under each circumstance are recorded. In Fig. 4(b), three typical curves are presented. These curves are in good accordance with each other that obviously reveals the grating's good polarization independency. The insets show the patterns

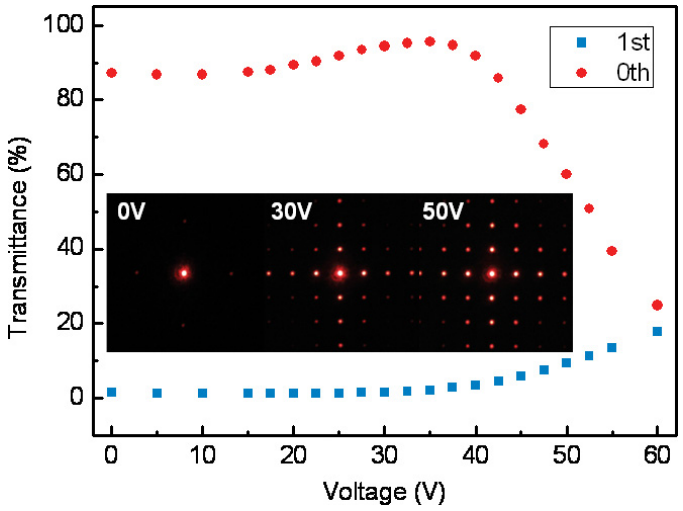

FIGURE 5 — Diffraction patterns (insets) and efficiencies of zeroth and first orders of 2D gratings.

taken at 40 V_{rms}, their highly similarity is coincident with the above results.

The behavior of the 2D gratings were measured as well. The voltage-dependent intensities of the zeroth and first orders are shown in Fig. 5, with a diffraction efficiency of the first order achieving 17.8% at 60 V_{rms}. The insets exhibit diffraction patterns at different applied voltages. There is one difference compared to the 1D case: The zeroth-order intensity increases along the applied voltages until 36 V_{rms}. The reason is considered to be the uniform orientation of the BP cubic lattices driven by the electric field, resulting in suppression of scattering and an increase in total transmittance. This agrees with the color changes of textures before and after applying a voltage as shown previously. However, a further increase in the applied voltages induces the redistribution of energy into diffraction orders, so the intensity decreases dramatically. Besides the mechanism of polarization independency described above, the geometrical symmetry further facilities the independency. Our results are in agreement.

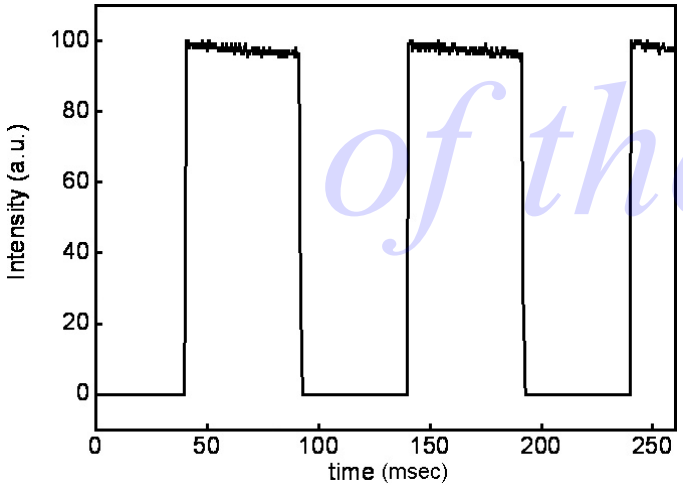

FIGURE 6 — Switching-on/off time of 1D BPLC grating.

The switching-on/off time, defined as 10–90% in transmittance and reverse of the presented grating was tested. Measured values were 380 and 860 μsec, respectively, calculated from Fig. 6. Both data are in the submillisecond range. The fast switching time permits the proposed gratings to be applied to a wide field of tunable optical elements and devices, such as optical interconnects, beam-steering devices, and spatial light modulators.

5 Conclusion

We propose a widely adaptable approach to form a tunable BPLC grating by applying a vertical electric field with lateral periodic distribution. Both 1D and 2D gratings with high efficiency, fast response time, and polarization independency were demonstrated. The simulation results support the predicted field distribution of alternating isotropic and ordinary refractive indices in the lateral direction. The performances can be further improved by optimization from both material and structure design aspects. This promising design brings potential wide applications in other fast-response photonics devices besides gratings, such as modulators, filters, attenuators, *etc.*

Acknowledgment

This work is sponsored by 973 programs (2011CBA00200 and 2012CB921803), the NSFJP program (BK2010360), the NSFC program (61108065), and the CPSF program (20110491370). The authors also thank the support from Infovision Optoelectronics Corporation, PAPD, and Fundamental Research Funds for the Central Universities. Correspondences regarding this paper should be addressed to Prof. Yan-qing Lu at yqlu@nju.edu.cn.

References

1 M. Schadt *et al.*, "Optical patterning of multidomain liquid-crystal displays with wide viewing angles," *Nature* **381**, No. 6579, 212–215 (1996).
2 S. T. Wu and C. S. Wu, "Mixed-mode twisted nematic liquid crystal cells for reflective displays," *Appl. Phys. Lett.* **68**, No. 11, 1455–1457 (1996).
3 X. Y. Zhu *et al.*, "Transflective liquid crystal displays," *J. Disp. Technol.* **1**, No. 1, 15–29 (2005).
4 Y. Q. Lu *et al.*, "Dual-frequency addressed hybrid-aligned nematic liquid crystal," *Appl. Phys. Lett.* **85**, No. 16, 3354–3356 (2004).
5 Y. H. Wu *et al.*, "Variable optical attenuator using polymer-stabilized dual-frequency liquid crystal," *Appl. Opt.* **44**, No. 20, 4394–4397 (2005).
6 Y. H. Lin *et al.*, "Polarization-independent liquid crystal phase modulator using a thin polymer-separated double-layered structure," *Opt. Express* **13**, No. 22, 8746–8752 (2005).
7 Y. H. Wu *et al.*, "Submillisecond response variable optical attenuator based on sheared polymer network liquid crystal," *Opt. Express* **12**, No. 25, 6382–6389 (2004).
8 H. W. Ren *et al.*, "Tunable-focus liquid lens controlled using a servo motor," *Opt. Express* **14**, No. 18, 8031–8036 (2006).
9 J. Feng *et al.*, "Fiber optic pressure sensor based on tunable liquid crystal technology," *IEEE Photonics J.* **2**, No. 5, 292–298 (2010).
10 X. W. Lin *et al.*, "Self-polarizing terahertz liquid crystal phase shifter," *AIP Advances* **1**, No. 3, 032133 (2011).

11 T. O. Carroll, "Liquid-crystal diffraction gratings," *J. Appl. Phys.* **43**, No. 3, 767–780 (1972).
12 L. L. Gu *et al.*, "Fringing-field minimization in liquid-crystal-based high-resolution switchable gratings," *Appl. Phys. Lett.* **87**, No. 20, 201106 (2005).
13 M. Bouvier and T. Scharf, "Analysis of nematic-liquid-crystal binary gratings with high spatial frequency," *Opt. Eng.* **39**, No. 8, 2129–2137 (2000).
14 R. G. Lindquist *et al.*, "High-resolution liquid-crystal phase grating formed by fringing fields from interdigitated electrodes," *Opt. Lett.* **19**, No. 9, 670–672 (1994).
15 J. Chen *et al.*, "An electro-optically controlled liquid crystal diffraction grating," *Appl. Phys. Lett.* **67**, No. 18, 2588–2590 (1995).
16 W. M. Gibbons and S.-T. Sun, "Optically generated liquid crystal gratings," *Appl. Phys. Lett.* **65**, No. 20, 2542–2544 (1994).
17 W. Hu *et al.*, "Liquid crystal gratings based on alternate TN and PA photoalignment," *Opt. Express* **20**, No. 5, 5384–5391 (2012).
18 R. L. Sutherland *et al.*, "Bragg gratings in an acrylate polymer consisting of periodic polymer-dispersed liquid-crystal planes," *Chem. Mater.* **5**, No. 10, 1533–1538 (1993).
19 Z. G. Zheng *et al.*, "Single-step exposure for two-dimensional electrically-tuneable diffraction grating based on polymer dispersed liquid crystal," *Liq. Cryst.* **35**, No. 4, 489–499 (2008).
20 Y. Q. Lu *et al.*, "Polarization switch using thick holographic polymer-dispersed liquid crystal grating," *J. Appl. Phys.* **95**, No. 3, 810–815 (2004).
21 H. Kikuchi *et al.*, "Polymer-stabilized liquid crystal blue phases," *Nature Mater.* **1**, No. 1, 64–68 (2002).
22 M. Z. Jiao *et al.*, "Low voltage and high transmittance blue-phase liquid crystal displays with corrugated electrodes," *Appl. Phys. Lett.* **96**, No. 1 (2010).
23 F. Zhou *et al.*, "A single-cell-gap transflective display using a blue-phase liquid crystal," *J. Display Technol.* **7**, No. 4, 170–173 (2011).
24 J. P. Cui *et al.*, "Transflective blue-phase liquid crystal display using an etched in-plane switching structure," *J. Display Technol.* **7**, No. 7, 398–401 (2011).
25 J. Yan *et al.*, "Polymer-stabilized optically isotropic liquid crystals for next-generation display and photonics applications," *J. Mater. Chem.* **21**, No. 22, 7870–7877 (2011).
26 Y. Li and S. T. Wu, "Polarization independent adaptive microlens with a blue-phase liquid crystal," *Opt. Express* **19**, No. 9, 8045–8050 (2011).
27 Y. H. Lin *et al.*, "Polarizer-free and fast response microlens arrays using polymer-stabilized blue phase liquid crystals," *Appl. Phys. Lett.* **96**, No. 11 (2010).
28 J. Yan *et al.*, "High-efficiency and fast-response tunable phase grating using a blue phase liquid crystal," *Opt. Lett.* **36**, No. 8, 1404–1406 (2011).
29 J. L. Zhu *et al.*, "1D/2D switchable grating based on field-induced polymer stabilized blue phase liquid crystal," *J. Appl. Phys.* **111**, 033101 (2012).
30 H. Stegemeyer *et al.*, "Thermodynamic, structural and morphological studies on liquid-crystalline blue phases," *Liq. Cryst.* **1**, No. 1, 3–28 (1986).
31 W. Y. Cao *et al.*, "Lasing in a three-dimensional photonic crystal of the liquid crystal blue phase II," *Nat. Mater.* **1**, No. 2, 111–113 (2002).
32 G. Zhu *et al.*, "Liquid crystal blue phase induced by bentshaped molecules with allylic end groups," *Opt. Mater. Express* **1**, No. 8, 1478–1483 (2011).
33 J. Yan *et al.*, "Extended Kerr effect of polymer-stabilized blue-phase liquid crystals," *Appl. Phys. Lett.* **96**, No. 7, 071105 (2010).
34 J. Kerr, "A new relation between electricity and light: Dielectrified media birefringent," *Philos. Mag.* **50**, No. 332, 337–348 (1875).

Wei Hu received his Ph.D. degree from Jilin University, Changchun, China, in 2009. He is currently a Lecturer at the College of Engineering and Applied Sciences and the National Laboratory of Solid State Microstructures, Nanjing University, Nanjing, China. His research is focused on liquid-crystal optical devices and novel liquid-crystal materials at the present time. He is an author or co-author of 20 journal papers, one book chapter, 12 conference presentations, and 12 patents and patent applications.

Zhi-gang Zheng received his Ph.D. degree from the Chinese Academy of Sciences in 2009. He then joined the East China University of Science and Technology (ECUST). Currently, he is working at the Materials Sciences Center of ECUST. His research interest involves new optically isotropic liquid-crystal materials and devices, light-sensitive liquid-crystal materials and devices, liquid-crystal/polymer composite, bent-core materials, molecular designing of liquid crystals, and liquid-crystal applications in the THz field. He has published more than 30 papers.

Yan-Qing Lu received his Ph.D. degree from Nanjing University, Nanjing, China, in 1996. He is currently a Professor at the College of Engineering and Applied Sciences and the National Laboratory of Solid State Microstructures, Nanjing University. He is the author or co-author of more than 100 peer-reviewed papers on optoelectronic materials and devices and holds 27 U.S. and China patents. His research interests include fiber optics, nanophotonics, and liquid-crystal devices.